

Auger recombination and intraband absorption of two-photon-excited carriers in colloidal CdSe quantum dots

Yingli Qu and Wei Ji^{a)}*Department of Physics, National University of Singapore, Singapore 117542, Republic of Singapore*

Yuanguang Zheng and Jackie Y. Ying

Institute of Bioengineering and Nanotechnology, Singapore 138669, Republic of Singapore

(Received 8 October 2006; accepted 16 February 2007; published online 29 March 2007)

Auger recombination, quantized Auger rate, and intraband absorption of two-photon-excited carriers in colloidal CdSe quantum dots have been investigated systematically with femtosecond Z scans and transient absorption measurements. The Auger constant is revealed to be on the order of $10^{-30} \text{ cm}^6 \text{ s}^{-1}$, while the intraband absorption cross sections are found to be in the range of $10^{-18} - 10^{-17} \text{ cm}^2$. The authors' experimental evidence demonstrates that the Auger recombination or the intraband absorption takes place under the condition that the average electron-hole pair per quantum dot is in excess of the unity. © 2007 American Institute of Physics.

[DOI: 10.1063/1.2716067]

Recently, fluorescent semiconductor nanocrystal quantum dots (QDs) have received tremendous attention due to their applications to two-photon microscopy.^{1–4} In such applications, radiative recombination of electron-hole ($e-h$) pairs, which follows two-photon absorption (TPA), are detected to form three-dimensional imaging, which has been reported to revolutionize bioimaging technology. A better understanding of two-photon excitation and relaxation processes therefore has important technological implication. In particular, studies should be carried out to gain insights into dynamical mechanisms which lead to a saturation in the overall efficiency of TPA-excited fluorescence (i.e., the ratio of the number of fluorescent photons to the total number of incoming photons). Such saturation has been observed.⁴ Here, we report a systematic study on both Auger recombination and intraband absorption of TPA-excited carriers in colloidal CdSe QDs, which contribute to saturation of TPA-excited fluorescence at high laser intensities.

As illustrated in Fig. 1(a), the Auger process, in which an $e-h$ pair is annihilated and another carrier (electron or hole) is excited to a higher energy level, may take place after a two-photon excitation. The Auger process is more efficient due to enhanced carrier-carrier interaction in the confined space of QDs in comparison with bulk materials.^{5–7} Although Auger recombination of one-photon-excited carriers in colloidal QDs has been studied intensively, no report is available in the literature for the case of two-photon excitation. Our investigation shows that the Auger process by two-photon excitation is as efficient as by one-photon excitation. More significantly, initial fast relaxations to the lowest states within the bands imply that the so-called “phonon bottleneck” is bypassed, contradicting the prediction^{8,9} but consistent with observations by one-photon excitation, though the initial excited states involved are different between one-photon and two-photon excitations.

Furthermore, we also analyze the intraband absorption of TPA-excited carriers in colloidal QDs. This process providing another channel for deteriorating the overall efficiency of

TPA-excited fluorescence at high laser intensities. Though the intraband absorption of TPA-excited carriers has been investigated in bulk semiconductors, similar effects in colloidal QDs have been largely overlooked.

The QDs studied here are semiconductor nanocrystal CdSe QDs coated with a layer of glutathione (GSH). The synthesis of GSH-capped CdSe QDs was based on the reaction of cadmium chloride with sodium hydroselenide (NaHSe). The high-resolution transmission electron microscopy (HRTEM) image in Fig. 1(b) shows both the dimension and crystalline structure of the QDs, which are 2.2 nm in diameter on average, with a standard deviation of 18% in the overall size of the QDs. The x-ray diffraction (XRD) data in Fig. 1(c) reveal the zinc blend cubic structure for the CdSe core.

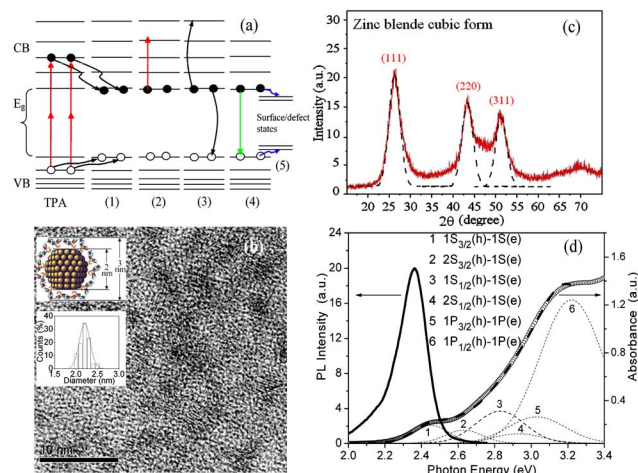


FIG. 1. (Color online) (a) Schematic diagram of TPA and subsequent relaxations. After TPA, the carriers decay through (1) intraband relaxation, (2) intraband absorption, (3) Auger process, (4) radiative recombination, or (5) trapping to surface/defect states. (b) HRTEM image of GSH-capped CdSe QDs; the insets show both the artistic impression and the size distribution. (c) XRD pattern of the QDs. The solid line is the XRD measurement. The dashed line is the fit with Gaussian curves. (d) Spectra of the one-photon absorption (circle) and one-photon-excited fluorescence excited at 350 nm (solid line) for the QDs in aqueous solution. The dashed curves are the theoretical fits.

^{a)}Electronic mail: phyjiwei@nus.edu.sg

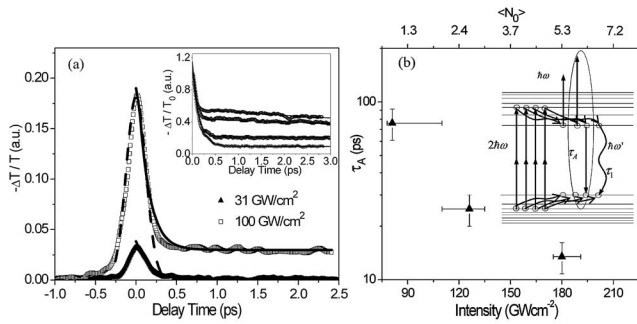


FIG. 2. (a) Transient absorption in aqueous solution of GSH-capped CdSe QDs measured with 120 fs laser pulses to a wavelength of 780 nm. The dashed curve is the autocorrelation between the pump and probe pulses. The inset shows the relaxation processes measured at various pump intensities of 180, 130, 80, and 65 GW cm⁻² (from the top down). At these pump intensities, two-photon-excited *e-h* pairs per QD are $\langle N_0 \rangle = 5.4, 2.6, 1.1$, and 0.7 , respectively. The solid lines for $\langle N_0 \rangle < 1$ are two-exponential fitting curves with $\tau_0 = 0.13$ ps and $\tau_1 > 300$ ps. The solid lines for $\langle N_0 \rangle > 1$ are fitted using the model of quantized decay steps and Poisson distribution for initial states. (b) Effective Auger relaxation time vs pump intensity or $\langle N_0 \rangle$. The triangles are the symbols for τ_A . The inset illustrates pathways for the relaxation of excited electrons or holes.

Figure 1(d) displays the spectra of one-photon absorption and one-photon-excited photoluminescence (PL) for the CdSe QDs in aqueous solution. The electronic structures of CdSe QDs have been investigated extensively, and there are several theories available in the literature.^{10,11} Based on the theoretical calculation reported in Ref. 11, we find that our measured absorption spectrum can be fitted well by taking into consideration several excitonic transitions with Gaussian broadening which correspond to the size dispersion mentioned above. The lowest excitonic transition is at 2.45 eV for CdSe QDs of 2.2 nm diameter, consistent with the experimental finding of Ref. 12. A blueshift of 750 meV is found in comparison with the band-gap energy of CdSe bulk crystal. The PL spectrum shows that the band-edge emission is centered at 2.36 eV with a full width at half maximum of ~ 200 meV.

TPA-excited carrier dynamics in the CdSe QD solution in 1-mm-thick quartz cuvette were investigated with 120 fs laser pulses. The wavelength tunable laser pulses were generated by an optical parametric amplifier (Quantronix, TOPS), which was pumped by a Ti:sapphire regenerative amplifier (Quantronix, Titan) at 1 kHz repetition rate. In our transient absorption measurements, a cross-polarized, pump-probe configuration was utilized. With the cross-polarized configuration, any “coherent artifact” on the transient absorption was eliminated. With 120 fs pulse duration and low pulse repetition rate (1 kHz), nonlinear absorption resulting from laser heating was found to be insignificant.

The pump-probe measurements in Fig. 2(a) demonstrate that the effect of TPA-excited carriers is negligible at low pump intensities (≤ 30 GW cm⁻²). Hence, the magnitude of TPA can be determined unambiguously from such Z scans. With the standard Z-scan theory for pure TPA,¹³ we extract the TPA coefficient of the CdSe QD solution from the best fit between the theoretical simulation and the Z scans. From the TPA coefficient, which is denoted as β , we infer the TPA cross section by $\sigma_{2PA} = \beta \hbar \omega / N$, where N is the number of QDs per cubic centimeter and $\hbar \omega$ is the photon energy. We plot σ_{2PA} as a function of $\hbar \omega / E_g$ in Fig. 3, showing that σ_{2PA} are in the range of $3 \times 10^{-47} - 2 \times 10^{-46}$ cm⁴ s/photon with an

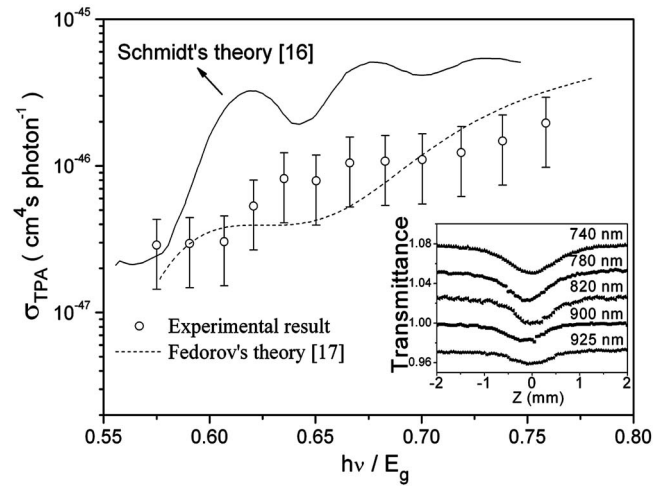


FIG. 3. Dispersion of the TPA cross section for GSH-capped CdSe QDs. The solid and dashed curves are the theoretical results. The inset shows Z scans measured at various wavelengths with laser intensities of 25 GW cm⁻² or less.

overall increase as the photon energy increases. The 2PA cross sections of CdSe QDs measured here are comparable to those of ZnS QDs,¹⁴ and are an order of magnitude greater than those of CdS QDs.¹⁵ With two-photon-excitation PL spectroscopy, Larson *et al.*⁴ determined the action cross sections $\phi_f \sigma_{2PA}$ to be on the order of 10^{-47} cm⁴ s/photon for colloidal CdSe QDs. If the fluorescence quantum efficiency ϕ_f is taken to be 40%, their TPA cross sections are in agreement with our findings. Theoretical works have been attempted for calculating the TPA cross sections of CdSe QDs.^{16,17} The measured TPA spectrum in Fig. 3 approaches the theoretical values of Fedorov *et al.*¹⁷ but the amplitude is five times smaller than the ones predicted by Schmidt *et al.*¹⁶ It should be emphasized that there is no ambiguity in our measurements, different from previously reported data^{4,15} which rely on ambiguous values of the fluorescence quantum efficiency.

With the accurate determination of the TPA coefficient discussed above, we can now precisely calculate the *e-h* pairs per QD. TPA-excited carrier density, N_{e-h} , is given by

$$dN_{e-h}/dt = \beta I^2 / (2\hbar\omega) - N_{e-h} / \tau_{\text{eff}}, \quad (1)$$

where τ_{eff} is the effective lifetime for TPA-excited carriers. τ_{eff} is much longer than the pulse duration, and the second item at the right side can be ignored. The density of TPA-excited carriers is given below with the assumption that the temporal and spatial profiles of laser pulse are Gaussian functions,

$$N_{e-h} = \frac{\beta I_0^2 \tau_G \sqrt{\pi}}{2\hbar\omega}, \quad (2)$$

where τ_G is the half-width at $1/e$ maximum for the pulse duration. I_0 is the on-axis intensity at the focus point of the Gaussian beam. With Eq. (2) we can accurately evaluate the average *e-h* pairs per QD, $\langle N_0 \rangle = N_{e-h} / N$, for a given pump intensity.

The effects of TPA-excited carriers in the CdSe QDs manifest themselves at pump intensities in excess of 50 GW cm⁻² ($\langle N_0 \rangle = 0.5$). As illustrated in Fig. 2(a), it is evident that at 100 GW cm⁻², a long tail appears in the transient signal, which is attributed to the presence of a significant

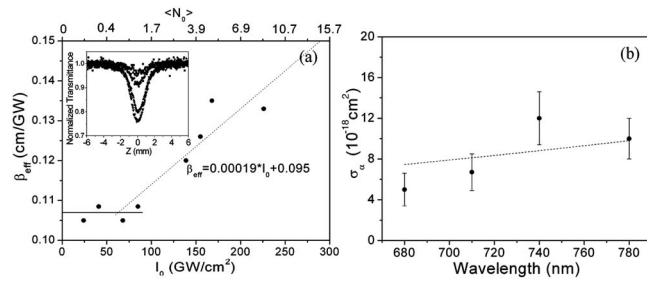


FIG. 4. (a) Effective TPA coefficient β_{eff} vs laser intensity or $\langle N_0 \rangle$. The filled circles are the extracted β_{eff} values from the Z scans. The inset shows several examples of Z scans at 780 nm with laser intensities of 24, 68, 139, and 168 GW cm^{-2} (from up to down). (b) σ_α vs laser wavelength. The dotted lines are the guideline for square dependence on wavelength.

density of TPA-excited carriers. To study more details, the inset of Fig. 2(a) displays the relaxation part of the transient absorption signal at different pump intensities. The relaxation process may be described quantitatively by using a three-exponential fitting: $A_0 e^{-t/\tau_0} + A_1 e^{-t/\tau_1} + A_2 e^{-t/\tau_A}$, where the fastest component, τ_0 , about 0.13 ps, is found to be independent of the pump intensity and is interpreted as the autocorrelation between the pump and probe pulses.¹⁸ The slowest component, τ_1 , on the nanosecond scale is attributed to radiative, band-to-band recombination.¹⁹ Note that the third time component τ_A is extremely sensitive to the pump intensity or the average e - h pairs in the QD. As shown in Fig. 2(b), τ_A are 13.5, 25, and 76 ps as $\langle N_0 \rangle = 5.4, 2.6$, and 1.1, respectively. If $\langle N_0 \rangle$ is less than 1, it disappears. This is consistent with the quantization of Auger recombination in QDs, which was first observed by Klimov *et al.*⁵ with one-photon excitation. To quantify it, Klimov *et al.* also developed a model of multiple e - h state decay through quantized steps: $dn_N/dt = -n_N/\tau_N$, $dn_{N-1}/dt = -n_{N-1}/\tau_{N-1} + n_N/\tau_N$, ... with the initial conditions for n_N, n_{N-1}, \dots, n_1 following Poisson distribution. With this model and the relationship²⁰ of $\tau_i/\tau_2 = (2/i)^2$ ($i > 2$), we extract $\tau_6 = 1.2$ ps, $\tau_5 = 1.7$ ps, $\tau_4 = 2.7$ ps, $\tau_3 = 4.8$ ps, and $\tau_2 = 10.8$ ps from the decay curves for $\langle N_0 \rangle = 5.4, 2.6$, and 1.1, and then conclude the Auger constant to be $\sim 1 \times 10^{-30} \text{ cm}^6 \text{ s}^{-1}$, which is in the same order of magnitude as the result obtained by Klimov *et al.* with one-photon excitation.⁵

In addition to the quantized Auger process, the intraband absorption of TPA-excited carriers is also observable by using Z scans in the regime of high laser intensities. After two-photon excitation, excited carriers relax quickly to the lowest energy state within the conduction (or valence) band in subpicosecond time scale due to the enhanced electron-hole energy transfer.²¹ At the same time, the two photon excited carriers may also make transitions instantaneously to higher energy states by absorbing another incoming photon. In this case, the reduction in the laser intensity I is given by

$$dI/dz = -(\alpha_0 + \beta I + \sigma_\alpha N_{e-h})I, \quad (3)$$

where α_0 is the linear absorption coefficient and σ_α is the intraband absorption cross section of TPA-excited carriers. Since N_{e-h} is proportional to the square of the laser intensity,

we derive an effective TPA coefficient, which comprises two parts: $\beta_{\text{eff}} = \beta + \Delta\beta$ and $\Delta\beta$, linearly dependent on the laser intensity. Indeed, our Z scans at high intensities in the inset of Fig. 4(a) permit us to extract the β_{eff} values, and then the plot of β_{eff} vs I_0 confirms the linear dependence, as illustrated in Fig. 4(a). When $\langle N_0 \rangle < 1$, the intraband absorption is insignificant, and thus β_{eff} is the intrinsic value for the TPA coefficient. By utilizing the Z-scan theory¹³ with both Eqs. (1) and (3), we simulate the Z-scan data measured at high intensities with σ_α being treated as one free parameter. The best fits allow us to unambiguously determine σ_α to be $\sim 10^{-17} \text{ cm}^2$ at 780 nm. Similar analytical procedures have been applied to the Z scans measured at wavelengths ranging from 680 to 760 nm. σ_α is shown to increase with wavelength in general in this wavelength range. The wavelength dependence of σ_α is displayed in Fig. 4(b), indicating that the intraband absorption is in qualitative agreement with Drude's model which predicts $\sigma_\alpha(\lambda) \propto \lambda^2$. Auger processes or surface state trappings occur in the time domain of a few picoseconds or longer. In our Z-scan experiments, we measured the intraband absorption within 120 fs. Hence, Auger processes or surface state trappings have little effect on our measurements.

¹X. Michalet, F. F. Pinaud, L. A. Bentolila, J. M. Tsay, S. Doose, J. J. Li, G. Sundaresan, A. M. Wu, S. S. Gambhir, and S. Weiss, *Science* **307**, 538 (2005).

²W. C. W. Chan and S. Nie, *Science* **281**, 2016 (1998).

³B. Dubertret, P. Skourides, D. J. Norris, V. Noireaux, A. H. Brivanlou, and A. Libchaber, *Science* **298**, 1759 (2002).

⁴D. R. Larson, W. R. Zipfel, R. M. Williams, S. W. Clark, M. P. Bruchez, F. W. Wise, and W. W. Webb, *Science* **300**, 1434 (2003).

⁵V. I. Klimov, A. A. Mikhailovsky, D. W. McBranch, C. A. Leatherdale, and M. G. Bawendi, *Science* **287**, 1011 (2000).

⁶M. Califano, A. Zunger, and A. Franceschetti, *Appl. Phys. Lett.* **84**, 2409 (2004).

⁷L. W. Wang, M. Califano, A. Zunger, and A. Franceschetti, *Phys. Rev. Lett.* **91**, 056404 (2003).

⁸U. Bockelmann and G. Bastard, *Phys. Rev. B* **42**, 8947 (1990).

⁹H. Benisty, C. Sotomayor-Torres, and C. Weisbuch, *Phys. Rev. B* **44**, 10945 (1991).

¹⁰A. D. Yoffe, *Adv. Phys.* **50**, 1 (2001), and references therein.

¹¹A. L. Efros and M. Rosen, *Annu. Rev. Mater. Sci.* **30**, 475 (2000).

¹²V. I. Klimov, *J. Phys. Chem. B* **104**, 6112 (2000).

¹³M. Sheik-Bahae, A. A. Said, T. H. Wei, D. J. Hagan, and E. W. V. Stryland, *IEEE J. Quantum Electron.* **26**, 760 (1990).

¹⁴V. V. Nikesh, A. Dharmadhikari, H. Ono, S. Nozaki, G. R. Kumar, and S. Mahamuni, *Appl. Phys. Lett.* **84**, 4602 (2004).

¹⁵J. W. M. Chon, M. Gu, C. Bullen, and P. Mulvaney, *Appl. Phys. Lett.* **84**, 4472 (2004).

¹⁶M. E. Schmidt, S. A. Blanton, M. A. Hines, and P. Guyot-Sionnest, *Phys. Rev. B* **53**, 12629 (1996).

¹⁷A. V. Fedorov, A. V. Baranov, and K. Inoue, *Phys. Rev. B* **54**, 8627 (1996).

¹⁸E. P. Ippen and C. V. Shank, in *Ultrashort Light Pulses, Picosecond Techniques and Applications*, edited by S. L. Shapiro (Springer, Berlin, 1977), Vol. 18, pp. 83–122.

¹⁹C. de Mello Donegá, M. Bode, and A. Meijerink, *Phys. Rev. B* **74**, 085320 (2006).

²⁰R. M. Kraus, P. G. Lagoudakis, J. Müller, A. L. Rogach, J. M. Lupton, and J. Feldmann, *J. Phys. Chem. B* **109**, 18214 (2005).

²¹A. L. Efros, V. A. Kharchenko, and M. Rosen, *Solid State Commun.* **93**, 281 (1995).